Accurate Eye Center Localization using Snakuscule

Sanyam Garg
Microsoft Research India
sanyamgarg93@yahoo.in

Abhinav Tripathi
Microsoft Research India
abhinavtripathi01@gmail.com

Edward Cutrell
Microsoft Research India
cutrell@microsoft.com

Abstract

Estimating eye centers is an important computer vision problem with several applications. In the past, eye center localization was constrained by the use of special hardware such as infrared cameras. Methods that estimate eye centers based on visible light have also been suggested in the literature, but these methods are inaccurate when used with low resolution images and wide ranges of lighting. We propose a novel method that can be used to detect eye centers efficiently, even with low resolution images provided by a webcam. Our method takes into consideration the circular nature of the iris and its intensity difference as compared to the sclera. It then uses an energy based active contour called Snakuscule for capturing the iris. We test our algorithm's robustness towards changes in pose, illumination and scale using the BioID database and Yale Face Database B. Our method compares well with existing state-of-the-art techniques in terms of accuracy, is easy to implement and exhibits real-time performance.

1. Introduction

Eye center localization is an important prerequisite for tasks such as gaze estimation [31], recognizing human emotions [6], face matching or recognition [21], and other applications in human computer interaction. Several techniques for eye center localization have been suggested in the literature and are broadly classified into three major groups [10]: (1) Electro Oculography; (2) Scleral search coil; and (3) Video and image processing techniques. In addition to image processing using visible light, infrared illumination has also been used for estimating eye centers [22]. However, all these techniques except for video-based methods using visible light either require dedicated and expensive hardware or equipment that must be worn by users [3, 14]. Appearance-based (non-infrared) eye locators have also been suggested [1, 2, 7, 9, 15, 18, 23, 28, 29, 30, 32] that can detect the eye regions without requiring any specialized hardware, but are not very accurate for tracking purposes. Approaches that combine techniques using visible light and infrared have also been suggested [34], but dedicated hardware is still required.

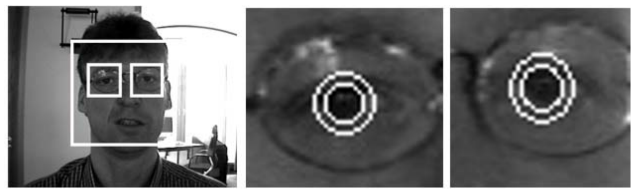

(a) (b) (c)

Figure 1: Detected face (a) and the eye center localization on extracted left and right eye regions (b and c)

Although infrared-based techniques can be very accurate, there are some situations in which closed up / infrared images may not be available. In such cases, methods using visible light may still be effectively utilized. Such methods can be divided into 4 major groups [13]: (1) Shape-based approaches; (2) Feature-Based Shape Methods; (3) Appearance Based Methods; and (4) Hybrid Models (combination of different methods). This paper describes a hybrid model for eye center localization using a non-deformable active contour that can accurately and quickly locate and track eye centers in low resolution images and videos that may be used in applications such as an eye gaze estimator using a laptop's webcam. Some methods that use deformable active contours for iris tracking using the Chan and Vese model [8] have been described in the literature [12, 16, 17]. However, due to their non-specific contour shape, numerous iterations need to be performed for minimizing the contour's energy before its final convergence, which is not suitable for real-time applications. We thus, describe a novel method for eye center localization wherein (1) we estimate the eye centers using an adaptive technique based on cumulative histograms; and (2) use an area-based circular snake called Snakuscule that captures the dark spherical iris surrounded by a lighter sclera. In the following section, the eye center estimation technique is explained. Section 3 provides the details of the Snakuscule algorithm. In Section 4, we test the accuracy and robustness of the proposed method for illumination and pose variations, and extensively compare the results with state-of-the-art systems for eye localization.

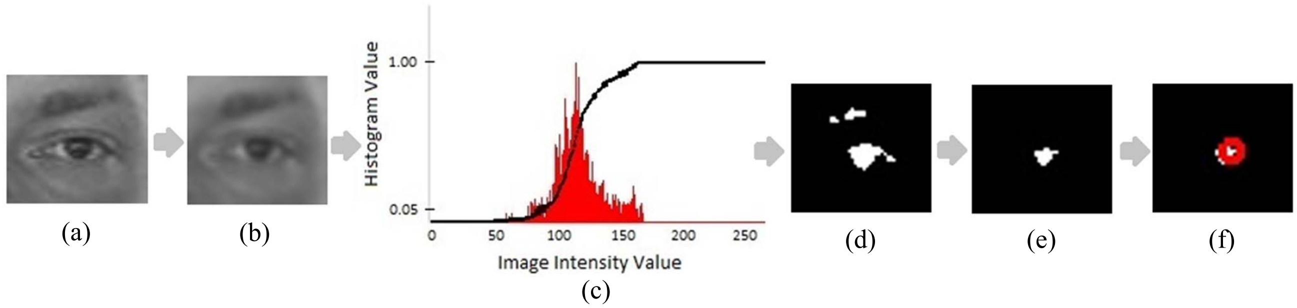

Figure 2: Procedure for iris segmentation. The Histogram of blurred eye image (b) is shown in red and Cumulative Histogram is shown in black (c). Figure (d) is obtained after adaptively thresholding image (b) using the Cumulative Histogram in (c). Erosion morphology is performed on Figure (d) to get Figure (e). The pixel with minimum intensity is marked in Figure (f).

2. Estimating Eye Center

To get a better understanding of the appearance of human eyes, we examined various individuals of different ethnicities and found that the iris is amongst the darkest circular regions of the eye. Yet, simple binary thresholding is not enough for segmenting the iris since many individuals also had dark eyebrows and eye lashes, and some wore eyeglasses with dark rims. Therefore, we utilized an adaptive approach for segmentation. A similar approach was suggested in [1]. We first used a multi-stage scheme for finding the eye regions wherein, the face position is first estimated by applying a boosted cascade face detector [33] and the eye positions are roughly extracted using anthropometric relations (Figure 1). Following this, the Cumulative Histogram M of the grayscale eye region for both the eyes is created by integrating their respective histograms m in the following way:

$$M_i = \sum_{j=0}^{i} m_j \text{ , } where\ 0 \le i \le 255 \quad (1)$$

where m_j denotes the probability of occurrence of gray level j. For the extracted eye region, we normalized the cumulative histogram and found that the iris and pupil have $M_i \le 0.05$, and thus, the iris region is segmented as:

$$I'(x, y) = \begin{cases} 255, & M_{i(x,y)} \le 0.05 \\ 0, & M_{i(x,y)} > 0.05 \end{cases} \quad (2)$$

A threshold of 0.04 did not segment the iris completely, while a threshold of 0.06 segmented the eyebrows significantly. The segmented image I' may still contain regions apart from the iris such as dark eyebrows, eye lashes etc. Hence, we eroded the segmented image with a structure element of kernel size 3x3 which performs better than the kernel size of 2x2 suggested in [1]. We also found that blurring the extracted eye image before finding the Cumulative Histogram improves the estimate of the eye centers. The entire procedure is illustrated in Figure 2.

Among all the segmented pixels (Figure 1(e)), we find the one with the least intensity and initialize the Snakuscule at that pixel location. Finding a good estimate of the eye center is a critical step to ensure that the Snakuscule converges in minimum number of iterations.

3. Snakuscule Initialization

Curve based geodesic active contours have been suggested previously for iris and pupil detection [24, 25], but would result in inaccuracies when implemented on low resolution images. Further, edge based snakes require sharp edges for efficient convergence. Energy based active contours without edges have also been used [12, 17] for iris segmentation, however employing a deformable active contour requires enormous number of iterations before final convergence thus making it unsuitable for real time performance. Since, iris is the most prominent circular region in an eye area and is characterized by its lower intensity as compared to the surrounding sclera, we initialize a shape-specific active contour called Snakuscule [27] for capturing the circular iris in the eye. This energy based active contour is non deformable and effectively tracks the eye in low resolution images. The low number of required iterations and real time performance is an added advantage.

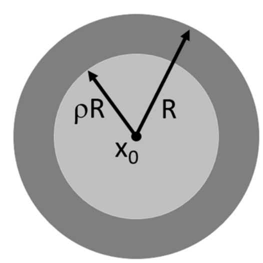

Figure 3: Structure of a Snakuscule

Snakuscule is an active circular boundary that moves under the influence of local energy gradients and once initialized on some part of the iris, it expands, contracts or moves so as to grab the iris completely. As a Snakuscule is circular in nature (Figure 3) it works best when detecting circular regions such as the iris. ρ (as shown in Figure 3) is defined as the ratio of inner to outer radius.

For eye center localization, we initialize a Snakuscule such that it overlaps with some part of the iris. For a

(a) (b)

Figure 4: Image showing the normalized energy values obtained by moving a Snakuscule in the entire eye image

Snakuscule, the energy difference between the outer annulus and the inner circle is calculated (Equation 3), and Snakuscule moves in the direction of decreasing energy difference. Out of the six possible movements, i.e. moving in four directions (Up, down, right, left), radius expansion and contraction, the Snakuscule chooses the one that provides the maximum decrease in its energy based on gradient descent. Energy to be minimized is given by the following equation:

$$\iint_{\rho R < \|x - x_o\| < R} f(x)\, dx_1\, dx_2 - \iint_{\|x - x_o\| < \rho R} f(x)\, dx_1\, dx_2, \quad (3)$$

where $f(x)$ is the image intensity at position x.

For the purpose of explaining how Snakuscule finds the iris accurately, we manually found the radius of the iris of the eye shown in Figure 4(a) and moved a Snakuscule in the entire eye image. At every position its energy was calculated and plotted. The normalized and inverted image of the energy values is shown in Figure 4(b). It is crucial to note that the Snakuscule had minimum energy at the eye center. An example of the Snakuscule initialization and final convergence is shown in Figure 5. In our research, we initialize the Snakuscule with an inner radius calculated on the basis of the dimensions of the bounding box of the eye-region and the radius thus calculated is a close approximation of the actual radius of the iris.

We introduce a new energy term (Equation 4) to restrict uncontrolled expansion or shrinkage of the active contour in presence of canonical gradients. The energy term given in Equation 3 was normalized by dividing the energy of outer annulus and inner disk by their respective areas. This enables us to create and test Snakuscules with different ρ values. The modified energy is given as:

$$\frac{\iint_{\rho R < \|x - x_o\| < R} f(x)\, dx_1\, dx_2}{\iint_{\rho R < \|x - x_o\| < R} dx_1\, dx_2} - \frac{\iint_{\|x - x_o\| < \rho R} f(x)\, dx_1\, dx_2}{\iint_{\|x - x_o\| < \rho R} dx_1\, dx_2} \quad (4)$$

where,

$$inner\ radius = \left(\frac{1}{\sqrt{\alpha}}\right) * outer\ radius, \alpha > 1 \quad (5)$$

We observed that $\alpha = 2.0$ (i.e. $\rho = 0.707$) provided a significant accuracy improvement compared to other α values.

Figure 5: The initialization and convergence of a Snakuscule (Best viewed in a color image)

4. Evaluations

In this section we test our proposed methodology on some complex image examples to evaluate the accuracy and robustness of our algorithm for variations in illumination, pose and scale. We later compare our results with state-of-the-art methods for eye center localization.

4.1 Evaluating accuracy using BioID Database

For evaluating the accuracy, we have used the BioID database [5]. The database consists of 1521 grayscale images of 23 different subjects which have been taken in different locations and daytimes. Besides changes in ambient light, the positions of the subjects vary in terms of both pose and scale. In many cases, the subjects are wearing glasses with dark rims, and some subjects have dark eyelashes. Furthermore, in quite a few cases, the subject's eyes are closed or are indistinguishable due to strong reflections on the eyeglasses. Because of such conditions, the BioID database is considered as one of the most challenging database available for testing purposes. The resolution of each image is 384x288.

Our proposed algorithm is applied on the extracted eye regions for every subject in the images, as demonstrated in Figure 1. We evaluate the *normalized error*, which is the error of the worse eye center estimation, as an indication of our algorithm's accuracy. This measure was suggested by Jesorsky *et al.* [15] and is defined as:

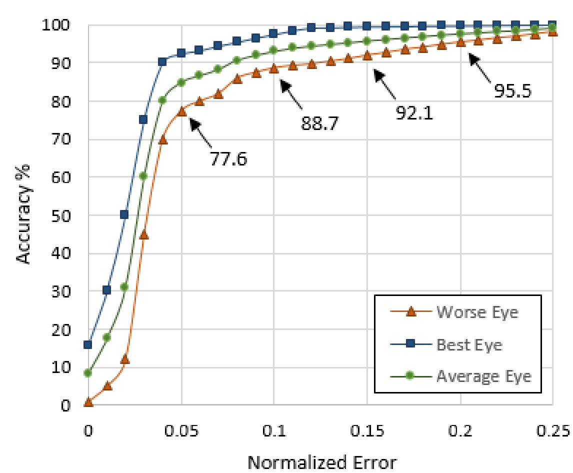

Graph 1: Accuracy vs. Normalized error for the worse, average and best eye obtained using the proposed method

Figure 6: Some examples of the results obtained on the images of BioID database. The first two rows show correct center estimation and the last row shows inaccurate results. The eye centers are marked with a white plus sign.

$$e = \frac{\max(|C_l - C_l'|, |C_r - C_r'|)}{|C_l - C_r|} \quad (6)$$

where C_l and C_r are the ground truth values and C_l' and C_r' are the estimated eye centers for the left and right eye respectively. Using this measure, different values of errors are classified into the following subgroups: (1) e ≤ 0.25 corresponds to the distance between the eye center and the corners, (2) e ≤ 0.10 corresponds to the diameter of the iris, and (3) e ≤ 0.05 corresponds to the diameter of the pupil. Thus, an accurate eye center detector should not just perform accurately for e ≤ 0.25 (indicating that the position of the detected center is in between the eye corners) but should also provide a good performance for e ≤ 0.05 (detected center is located within the pupil region).

The results obtained on the BioID database are shown qualitatively in Figure 6. It can be observed that our method successfully locates the eye center not only for images containing clearly visible pupils, but also in presence of eyeglasses, shadows, poor contrast, and thick eyelashes. The method also deals effectively with slight variations in pose and scale. By analyzing the failures shown in Figure 6 (last row), we find that the method produces inaccurate results when eyes are closed, when reflections on the eyeglasses obscure the eye, or when the eyebrows are thick and dark compared to the pupil, in which case the Snakuscule gets initialized at an incorrect location.

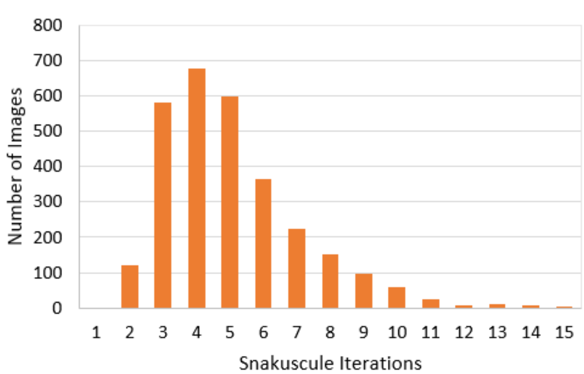

Graph 2: The number of images of BioID database for which the Snakuscule converged in given number of iterations

Graph 1 shows the quantitative accuracy obtained by our method on the BioID database. Using Equation 6, our method yields an accuracy of 77.6% for e ≤ 0.05 (pupil localization), which indicates a high probability of accurate center estimation within the pupil region. For e ≤ 0.10 (iris localization) our method produces a high accuracy of 88.7%. We also plot the *minimum normalized error* and the *average error*.

As an indication of the processing speed, we measured the number of iterations performed by the Snakuscule before final convergence, the results of which are plotted in Graph 2. We found that in more than 60% of the images, the Snakuscule converged in less than or equal to 4 iterations.

4.2 Evaluating robustness to Illumination and Pose changes using Yale Face Database B

To evaluate the robustness of our proposed method to lighting and pose variations, we use the Yale Face Database B [20]. The database contains 5760 single light source images of 10 subjects each seen under 576 viewing conditions (9 poses x 64 illumination conditions). The

Figure 7: Some sample images of the results obtained for different illumination conditions on a subject of the Yale Face Database B

Figure 8: Some sample images of the results obtained for different poses of subjects in the Extended Yale Face Database B.

resolution of each image is 640x480. To check the robustness of our method to illumination changes, the eye center localization method is tested only on frontal faces with changing illumination (10 subjects x 64 illuminations). The first two rows in Figure 7 show the results obtained for different illuminations on frontal faces qualitatively.

Investigating the results, we found that our system can handle illumination variations arising from different light source directions which can be as large as ±60° azimuthal and ±40° elevation with respect to the camera axis. For these particular angles, we recorded an accuracy of 81% (for $e \leq 0.05$), 89% (for $e \leq 0.10$) and 95% (for $e \leq 0.25$). Our method fails when extremely dark shadows are casted due to the nose as eye center is no longer the darkest region. For larger angles, the method works well for the more illuminated eye and is less robust in presence of extremely dark shadows. Even in cases of shadows appearing on the eye region, the method works effectively if the eye center is estimated correctly.

To estimate our method's performance on variations in pose, we use the Extended Yale Face Database B [11] which contains 16128 images of 28 human subjects under 9 poses and 64 illumination conditions. The images are of similar resolution as the Yale Face Database B. The pose angle varies up to 24 degrees from the camera optical axis. We choose a subset of the database images with ambient illumination (28 subjects x 9 poses) and test our method on them. The results are shown in Figure 8. Since the ground truth annotations for the eye centers are not available, we manually evaluated the results and achieved 98.2% accuracy for $e \leq 0.10$ which can be attributed to the presence of ambient light and absence of eye glasses. Furthermore, our method achieves 100% accuracy for $e \leq 0.10$ when an eye detector (Haar feature-based cascade classifier) is used in addition as it provides with a tighter bounding box for the eye region.

4.3 Comparison with State of the Art

We extensively compare our results with other state of the art methods suggested in literature that also used BioID database to test their algorithm. The comparison between our method and other state of the art methods is shown in Table 1 for different normalized errors 'e' values. The accuracy results have been obtained from the authors' papers or have been taken directly from their performance graphs.

The technique suggested by Asteriadis *et al.* [2] assigns a vector to every pixel in the eye region pointing towards the nearest edge pixel. Asadifard and Shanbezadeh [1] use Cumulative Distribution Function for finding the eye

Method	Accuracy ($e \leq 0.05$)	Accuracy ($e \leq 0.1$)	Accuracy ($e \leq 0.25$)
Asadifard [1] *	47	86	96
Asteriadis [2] *	74	81.7	97.4
Behnke [4]	37	86	98
Campadelli [7]	62	85.2	96.1
Cristinacce [9]	57	**96**	97.1
Jesorsky [15]	38	78.8	91.8
Kroon [18]	65	87	96
Leo [19]	80.67	87.31	94
Niu [23]	75	93	97
Timm [28] *	82.5	93.4	98.00
Turkan [29]	18.6	73.7	**99.6**
Valenti [32]	**86.09**	91.67	97.87
Valenti [32] *	81.89	87.05	98.00
Our method *	**77.6**	**88.7**	**98.6**

Table-1: Comparison of accuracy vs. normalized error for different methods on the BioID database.
*Methods that involve no learning based technique

center. Behnke [4] suggested the use of hierarchical neural networks with recurrent connectivity for eye center detection. Campadelli *et al.* [7] use two SVMs trained using Haar wavelet coefficients. Cristinacce *et al.* [9] used Pairwise Reinforcement of Feature Responses (PRFR) and Active Appearance Model (AAM) for further refinement. Leo *et al.* [19] combine the differential analysis of intensities of eye image with local variability of the appearance represented by self-similarity coefficients. Niu *et al.* [23] use two separate cascade classifiers and obtain accuracy using a two direction bootstrap strategy. Timm and Barth [28] find eye center by utilizing the dot products of image gradients. Turkan *et al.* [29] use a high pass wavelet transform and an SVM classifier on edge candidates for accurate estimation. Valenti and Gevers [32] use isophote properties to gain invariance to linear lighting conditions. They further use a scale space pyramid to gain scale invariance.

On comparison, we find that our method outperforms most of the previous suggested methods in the literature, though Valenti and Gevers's method [32] performs better for $e \leq 0.05$. However, they use techniques like nearest neighbour classifier, mean shift clustering and SIFT features which are not suitable for eye tracking in videos with several frames per second. Our method, on the other hand, requires no training and needs significantly less computation. For $e \leq 0.10$, our method performs reasonably well and is again comparable to other training based methods except for the one suggested by Cristinacce et al. [9], which can be justified by the fact that their method finds the eye corners using facial feature detectors. The improvement again comes at an expense of increased computational time as compared to our method that relies only on the intensity and circularity of the iris. For normalized error $e \leq 0.25$, our method achieved accuracy comparable to all other methods suggested in the literature.

Figure 9: Sample images demonstrating the robustness of the tracking procedure on Talking Face video

4.4 Eye Center Tracking in a Video

It was important to understand how our method would perform when run on a video with a high frame rate. Hence, we used the publicly available Talking Face video [26] which comprises of 5000 frames taken from a video of 200 seconds of a person engaged in a conversation. The resolution of each frame is 720x576.

For the very first frame, we initialize the eye tracker wherein we extract the eye region from the detected face and find Snakuscule's energy upon convergence using Equation 3. The position and radius of the converged Snakuscule in the previous frame is used for initializing a new Snakuscule in every subsequent frame. Also, we re-initialize the eye tracker whenever there is a drastic change in the energy of the Snakuscule between two consecutive frames (we found that an energy difference of 2 grayscale units gives accurate results). Moreover, the eye tracker is re-initialized every 20 frames.

Some sample images of the eye tracking results are shown in Figure 9. Using the tracker, we obtain an accuracy of 81% for $e \leq 0.05$ and 96.4% for $e \leq 0.10$. The low accuracy for $e \leq 0.05$ could be explained by the fact that the human annotations for the eye centers are sometimes unreliable in the Talking Face video. This negatively impacts the tracker's accuracy.

5. Discussions

It is critical that eye tracking algorithms are quick and accurate so that they can be employed for real time video processing. Our method depends upon an initial estimate of the eye center followed by multiple iterations of the Snakuscule until it converges. The eye center estimation requires inexpensive techniques such as histogram creation and image erosion which is linear in the size of the image. Calculating Snakuscule energy requires scanning through all its constituent pixels which is computationally insignificant due to its small radius in comparison to the extracted eye image size. For an image with resolution 320x240, our method takes 55ms for total computation on a single core 3.00GHz Intel Core 2 Duo processor. This roughly corresponds to 19FPS which is reasonably quick and can be used in real time applications.

6. Conclusion

We present an eye center localization method using energy based circular active contour called Snakuscule. The Snakuscule once initialized on some part of the iris, moves around to decrease its energy until it converges and captures the iris completely. The use of Snakuscule provides a computationally inexpensive method that is invariant to scale, pose and illumination changes. A cumulative histogram based adaptive thresholding method is used to further increase the accuracy as a base-line eye localization method.

We evaluate our method's accuracy and robustness on more than 2000 images. We further demonstrate the effectiveness of our method by comparing it against previous state of the art methods. Given the ease of implementation and the accuracy obtained, we believe that our method can be successfully adopted in real time applications which require a good estimate of the eye center in low resolution images.

Acknowledgements

This work would not have been possible without the assistance and insight provided by William Thies. We are grateful to Nakull Gupta, Andrew Cross, Danish Pruthi, Prem Parekh, Shruti Rijhwani, Sumit Sharma and Pranav Ramarao for their help. Finally, we would like to thank the reviewers for their helpful suggestions regarding this paper.

References

[1] M. Asadifard and J. Shanbezadeh. Automatic adaptive center of pupil detection using face detection and CDF analysis. IMECS, 2010.

[2] S. Asteriadis, N. Nikolaidis, A. Hajdu, and I. Pitas. An eye detection algorithm using pixel to edge information. In Int. Symp. on Control, Commun. and Sign. Proc, 2006.

[3] J. S. Babcock, J. Pelz. Building a lightweight eyetracking headgear. Proceedings of the 2004 symposium on Eye tracking research & applications, 109-114, 2004.

[4] S. Behnke. Learning face localization using hierarchical recurrent networks. ICANN, LNCS, 135–135. Springer, 2002.

[5] BioID Technology Research. The BioID Face Database. http://www.bioid.com, 2001.

[6] M. G. Calvo and P. J. Lang. Gaze Patterns When Looking at Emotional Pictures: Motivationally Biased Attention. Motivation and Emotion, Vol. 28(3): 221-243, September 2004.

[7] P. Campadelli, R. Lanzarotti, and G. Lipori. Precise eye localization through a general-to-specific model definition. BMVC, Vol I, 187–196, 2006.

[8] T.F. Chan and L.A. Vese. Active contours without edges. IEEE Transcations on Image Processing, Vol. 10(2), Feb 2001.

[9] D. Cristinacce, T. Cootes, and I. Scott. A multi-stage approach to facial feature detection. In BMVC, 277–286, 2004.

[10] A. T. Duchowski, Eye Tracking Methodology: Theory and Practice, Springer 2003.

[11] A. Georghiades, P. Belhumeur, D. Kriegman. From few to many: Illumination cone models for face recognition under variable lighting and pose. PAMI, Vol. 23(6): 643–660, 2001.

[12] A. Hilal, B. Daya and P. Beauseroy. Hough Transform and Active Contour for Enhanced Iris Segmentation. IJCSI, Vol. 9(6), Nov 2012.

[13] D. W. Hansen and Q. Ji. In the eye of the beholder: A survey of models for eyes and gaze. IEEE Trans. on PAMI, 32(3): 478–500, 2010.

[14] EL Irving, JE Zacher, RS Allison, ME Callender. The effects of scleral search coil wear on visual function. Invest Ophthalmol Vis Sci. Vol. 44(5), May 2003

[15] O. Jesorsky, K. J. Kirchberg and R. Frischholz. Robust face detection using the Hausdorff distance. In Audio and Video Biom. Pers. Auth., 90–95, 1992.

[16] R. Jillela, A. Ross, V.N. Boddeeti, B.V. Kumar, X. Hu, R. Plemmons, P. Pauca. An Evaluation of Iris Segmentation Algorithms in Challenging Periocular Images, in Handbook of Iris Recognition, K. Bowyer and M. Burge (Eds.), Springer 2013.

[17] J. Koh, V. Govindraju and V. Choudhary. A Robust Iris Localization Method Using an Active Contour Model and Hough Transform. International Conference on Pattern Recognition. 2010.

[18] B. Kroon, A. Hanjalic, and S. Maas. Eye localization for face matching: is it always useful and under what conditions? CIVR, 379–388. ACM, 2008.

[19] M. Leo, D. Cazzato, T.D. Marco, C. Distante. Unsupervised Eye Pupil Localization through Differential Geometry and Local Self-Similarity Matching. PLOS One, 2014.

[20] K.C. Lee, J. Ho, and D. Kriegman, Acquiring Linear Subspaces for Face Recognition under Variable Lighting, IEEE Trans. PAMI, Vol. 27(5), 2005.

[21] N.N. Maw, M. Pomplun. Studying Human Face Recognition with the Gaze-Contingent Window Technique. Cognitive Science Society, 927-932, 2004.

[22] C.H. Morimoto, M. R. M. Mimica, Eye gaze tracking techniques for interactive applications, CVIU, 98(1), 2005.

[23] Z. Niu, S. Shan, S. Yan, X. Chen, and W. Gao. 2D cascaded adaboost for eye localization. ICPR, Vol. 2, 1216– 1219, 2006

[24] A. Ross and S. Shah, Segmenting Non-Ideal Irises Using Geodesic Active Contours. BSYM, 2006.

[25] S. Shah and A. Ross. Iris Segmentation Using Geodesic Active Contours. IEEE Transactions on Information Forensics and Security, Vol 4(4), 824-836, 2009.

[26] Talking Face Video. Face&Gesture Recognition Working group, IST-2000-26434, http://www-prima.inrialpes.fr/FGnet/ data/01-TalkingFace/talking_ face.html

[27] P. Thevenaz and M.Unser. Snakuscules. IEEE Trans. Image Proc. Vol. 17(4): pp. 585-593, April 2008.

[28] F. Timm and E. Barth. Accurate eye centre localisation by means of gradients. VISAPP, 2011

[29] M. Turkan, M. Pardes, and A. E. Cetin. Human eye localization using edge projections. VISAPP, 410–415. 2007.
[30] R. Valenti and T. Gevers. Accurate eye center location and tracking using isophote curvature. CVPR, 2008.
[31] R. Valenti, N. Sebe and T. Gevers. Combining Head Pose and Eye Location Information for Gaze Estimation. IEEE Trans. on Image Processing, Vol 21(2), Feb 2012.
[32] R. Valenti and T. Gevers. Accurate Eye Center Location through Invariant Isocentric Patterns, IEEE Trans. on PAMI. Vol 34(9), 1785-1798, Sep 2012.
[33] P. Viola and M. Jones. Robust real-time face detection. IJCV, 57(2): 137–154, 2004.
[34] Z. Zhu and Q. Ji. Robust real-time eye detection and tracking under variable lighting conditions and various face orientations. CVIU, Vol. 98(1): 124–154, 2005.